

Study of Clustered Robust Linear Precoding for Cell-Free MU-MIMO Networks

André R. Flores¹ and Rodrigo C. de Lamare^{1,2}

¹Centre for Telecommunications Studies, Pontifical Catholic University of Rio de Janeiro, Brazil

²Department of Electronic Engineering, University of York, United Kingdom

Emails: {andre_flores, delamare}@puc-rio.br

Abstract—Precoding techniques are key to dealing with multiuser interference in the downlink of cell-free (CF) multiple-input multiple-output systems. However, these techniques rely on accurate estimates of the channel state information at the transmitter (CSIT), which is not possible to obtain in practical systems. As a result, precoders cannot handle interference as expected and the residual interference substantially degrades the performance of the system. To address this problem, CF systems require precoders that are robust to CSIT imperfections. In this paper, we propose novel robust precoding techniques to mitigate the effects of residual multiuser interference. To this end, we include a loading term that minimizes the effects of the imperfect CSIT in the optimization objective. We further derive robust precoders that employ clusters of users and access points to reduce the computational cost and the signaling load. Numerical experiments show that the proposed robust minimum mean-square error (MMSE) precoding techniques outperform the conventional MMSE precoder for various accuracy levels of CSIT estimates.

Index Terms—Cell-free wireless networks, cluster precoders, MIMO, multiuser interference, robust precoding.

I. INTRODUCTION

Cellular networks today rely on coordinated base stations (BSs) deployed to cover an extensive area and provide a variety of services to the users. Future applications of wireless communications require cellular networks to offer higher throughput [1], [2], [3], [4]. Since further densification of BSs is impractical, cell-free (CF) multiple-input multiple-output (MIMO) systems have emerged as an attractive alternative to improve the overall performance and support future applications [5], [6]. Unlike BS-based networks, CF-MIMO employs multiple access points (APs) distributed over the area of interest. The APs are coordinated by a central processing unit (CPU) located at the cloud server. This distributed deployment has benefits such as increased throughput per user [7], [8], [5], [9], [10] as well as better energy efficiency [11], [12], [13] when compared with the conventional BS-based networks.

To fully harness the benefits of CF-MIMO systems in the downlink and handle multiuser interference (MUI), precoding techniques [14], [15], [16], [17], [18], [19], [20], [21], [22], [23], [24], [25], [26], [27], [28], [29], [30], [31], [32] are employed. Linear precoding such as matched filter (MF), zero-forcing (ZF) [33], and minimum mean-square error (MMSE) [34] precoders are widely used in CF MU-MIMO. Initially, these techniques were employed as network-wide (NW) precoders [35], [33]. But NW precoders are not practical because

they involve extremely high signaling loads and computational cost.

To address the problems with traditional NW precoders, several studies recommend to employ a reduced set of APs and users [36], [37], [38]. Following this technique, NW precoders have evolved to precoders that employ APs and user clustering [39], [36], [40] to address the high computational complexity of NW precoders. In [39], the number of APs is reduced to make better use of the resources and diminish the signaling load. Scalable MMSE combiners are derived along with precoders by exploiting the uplink-downlink duality in [36]. A regularized ZF precoder is proposed in [40], where several subsets are formed to reduce the number of APs serving each user. In [41], clusters of users and APs are formed to reduce the overall computational complexity.

Another major problem with precoding techniques is that they assume perfect knowledge of the channel state information at the transmitter (CSIT). In practice, such assumption is hardly verified and residual multiuser interference degrades the performance of precoding techniques [42]. As a result, there is a demand for robust precoding techniques that are tolerant of imperfect CSIT. Robust precoders were initially developed in sensor array signal processing, wherein some well-established methods included diagonal loading [43], generalized loading [44], and worst case optimization [45]. Moreover, a non-conventional transmit scheme known as rate-splitting has been developed to enhance the robustness of the system, [46], [47]. A low complexity robust precoder with per antenna power constraint was proposed in [48]. Furthermore, a robust MMSE precoding scheme with power allocation was developed in [24]. However, the computational cost of the technique in [24] is high because it employs NW precoders and requires searching the precoder parameter.

In this paper, contrary to previous studies, we propose a robust MMSE precoders to mitigate the negative effects of MUI through alternating optimization of the precoder and the regularization parameter. We also introduce sparse and cluster-based robust precoders to enhance the overall performance while keeping the computational cost low. In both cases, we perform AP selection to reduce the amount of signaling required. The cluster-based robust precoders employ clusters of users to reduce the computational load. Numerical experiments show that the proposed robust techniques outperforms existing precoders.

The rest of this paper is organized as follows. In the next section, we present the system model of the downlink of a CF MIMO. In Section III, we derive the proposed robust MMSE-based precoding algorithms. We introduce the sum-rate as a performance metric in Section IV and validate our methods through numerical experiments in Section V. We conclude in Section VI.

Throughout this paper, we reserve the bold lowercase, bold uppercase, and calligraphic letters for vectors, matrices, and sets, respectively; the notations $(\cdot)^T$, $(\cdot)^H$, $(\cdot)^*$, $\|\cdot\|$ and $|\cdot|$ stand for the transpose, Hermitian, complex conjugate, Euclidean norm, and magnitude, respectively; $\text{Tr}(\cdot)$ and $\mathbb{E}[\cdot]$ represent trace and statistical expectation operators, respectively. The operator $\Re\{\cdot\}$ retains the real part of a complex argument. An $N \times K$ matrix with column vectors $\mathbf{a}_1, \dots, \mathbf{a}_K$, each of length N , is $\mathbf{A} = [\mathbf{a}_1, \dots, \mathbf{a}_K]$.

II. SYSTEM MODEL

Consider the downlink of a CF MIMO system operating with N APs distributed over the area of interest. The system provides service to a total of K users, each one equipped with a single omnidirectional antenna. A central processing unit (CPU) located at the cloud server is connected to the APs. The data are transmitted over a flat-fading channel $\mathbf{G}^T \in \mathbb{C}^{K \times N}$. The (n, k) -th element of matrix \mathbf{G} is the channel coefficient between the n -th AP and k -th user, i.e., $g_{n,k} = \sqrt{\zeta_{n,k}} h_{n,k}$, where $\zeta_{n,k}$ is the large-scale fading coefficient that models the path loss and shadowing effects, and $h_{n,k}$ represents the small-scale fading coefficient. The coefficients $h_{n,k}$ are modeled as independently and identically distributed (i.i.d.) random variables with complex Gaussian distribution $\mathcal{CN}(0, 1)$.

Denote the transmit signal by $\mathbf{x} \in \mathbb{C}^N$, which obeys the transmit power constraint $\mathbb{E}[\|\mathbf{x}\|^2] \leq P_t$, where $\mathbb{E}[\cdot]$ denotes the statistical expectation. Then, the $K \times 1$ received signal vector is

$$\mathbf{y} = \mathbf{G}^T \mathbf{x} + \mathbf{n}, \quad (1)$$

where $\mathbf{n} \in \mathbb{C}^K$ is the additive white Gaussian noise (AWGN) that follows the distribution $\mathcal{CN}(\mathbf{0}, \sigma_n^2 \mathbf{I})$. The transmitted signal is

$$\mathbf{x} = \mathbf{P} \mathbf{s} = \sum_{k=1}^K s_k \mathbf{p}_k, \quad (2)$$

where the vector of symbols $\mathbf{s} = [s_1, s_2, \dots, s_K]^T \in \mathbb{C}^K$ contains the information intended to the users and the precoding matrix $\mathbf{P} = [\mathbf{p}_1, \mathbf{p}_2, \dots, \mathbf{p}_K] \in \mathbb{C}^{N \times K}$, where \mathbf{p}_k is its k -th column, maps the symbols to the transmit antennas.

The system employs the time division duplexing (TDD) protocol and, therefore, the channels are estimated by leveraging upon the channel reciprocity property and pilot training [42]. After receiving the pilots, the CPU computes the channel estimate $\hat{\mathbf{G}}^T = [\hat{\mathbf{g}}_1, \hat{\mathbf{g}}_2, \dots, \hat{\mathbf{g}}_K]^T \in \mathbb{C}^{K \times N}$. The (n, k) -th element of matrix $\hat{\mathbf{G}}$ is

$$\hat{g}_{n,k} = \sqrt{\zeta_{n,k}} \left(\sqrt{1 + \sigma_e^2} h_{n,k} - \sigma_e \tilde{h}_{n,k} \right), \quad (3)$$

where the variable $\hat{g}_{n,k}$ denotes the channel estimate between the n -th AP and the k -th user, $\tilde{h}_{n,k}$ is i.i.d $\mathcal{CN}(0, 1)$ (independent from $h_{n,k}$) and models the error in the channel estimate, and σ_e represents the quality of the channel state information (CSI). The error affecting the channel estimate $\hat{g}_{n,k}$ is denoted by $\tilde{g}_{n,k} = \sigma_e \sqrt{\zeta_{n,k}} \tilde{h}_{n,k}$, which is the (n, k) -th coefficient of the error matrix $\tilde{\mathbf{G}}$.

A. Robust MMSE

We consider an extended objective function which mitigates the effects of the imperfect CSIT. To this end, define the channel as $\mathbf{G}^T = \frac{1}{\tau} (\hat{\mathbf{G}}^T + \tilde{\mathbf{G}}^T)$, where $\tau = \sqrt{1 + \sigma_e^2}$. Then, the received signal is

$$\mathbf{y} = \frac{1}{\tau} \hat{\mathbf{G}}^T \mathbf{P} \mathbf{s} + \underbrace{\frac{1}{\tau} \tilde{\mathbf{G}}^T \mathbf{P} \mathbf{s}}_{\Delta} + \mathbf{n}. \quad (4)$$

The optimal precoder would minimize the effect of the imperfect CSIT (e.g., by letting $\mathbb{E}[\|\Delta\|^2] \rightarrow 0$) and perform as close as possible to the perfect CSIT case. To find such a precoder, we consider solving the following optimization problem

$$\begin{aligned} \{\mathbf{P}, f\} = \text{argmin} \quad & \underbrace{\mathbb{E}[\|\mathbf{s} - f^{-1} \mathbf{y}\|^2]}_{T_1} + \mathbb{E}[\|\Delta\|^2] \\ \text{subject to} \quad & \mathbb{E}[\|\mathbf{x}\|^2] = \text{tr}(\mathbf{P} \mathbf{P}^H) = P_t, \end{aligned} \quad (5)$$

where $\text{tr}(\cdot)$ is the trace of its matrix argument and f is a normalization factor that can be interpreted as an automatic gain control at the receivers [49], [24]. The following Proposition 1 provides the solution to this optimization problem

Proposition 1. *The robust precoder $\mathbf{P}^{(r)}$ that solves (5) is*

$$\mathbf{P}^{(r)} = f_r \bar{\mathbf{P}}, \quad (6)$$

where

$$\bar{\mathbf{P}} = \underbrace{(\hat{\mathbf{G}}^* \hat{\mathbf{G}}^T + \mathbb{E}[\tilde{\mathbf{G}}^* \tilde{\mathbf{G}}^T] + f^2 \mathbb{E}[\tilde{\mathbf{G}}^* \tilde{\mathbf{G}}^T] + \lambda f_r^2 \mathbf{I})^{-1} \hat{\mathbf{G}}^*}_{\mathbf{P}^{(i)}}, \quad (7)$$

assuming that the inverse of $\mathbf{P}^{(i)}$ exists.

Proof: We have the mean squared error

$$\begin{aligned} \mathbb{E}[\|\mathbf{s} - f^{-1} \mathbf{y}\|^2] = & \underbrace{\mathbb{E}[\mathbf{s}^H \mathbf{s}]}_{T_{11}} - f^{-1} \underbrace{\mathbb{E}[\mathbf{s}^H \mathbf{y}]}_{T_{12}} \\ & - f^{-1} \underbrace{\mathbb{E}[\mathbf{y}^H \mathbf{s}]}_{T_{13}} + f^{-2} \underbrace{\mathbb{E}[\mathbf{y}^H \mathbf{y}]}_{T_{14}}. \end{aligned} \quad (8)$$

Expanding the second term of (8) produces

$$T_{12} = \frac{1}{\tau} \left[\text{tr}(\hat{\mathbf{G}}^T \mathbf{P}) + \text{tr}(\mathbb{E}[\tilde{\mathbf{G}}^T] \mathbf{P}) \right]. \quad (9)$$

Similarly, the third term of (8) is

$$T_{13} = \frac{1}{\tau} \left[\text{tr}(\mathbf{P}^H \hat{\mathbf{G}}^*) + \text{tr}(\mathbf{P}^H \mathbb{E}[\tilde{\mathbf{G}}^*]) \right]. \quad (10)$$

Evaluating T_{14} yields

$$T_4 = \frac{1}{\tau^2} \left[\text{tr} \left(\mathbf{P} \mathbf{P}^H \tilde{\mathbf{G}}^* \hat{\mathbf{G}}^T \right) + \text{tr} \left(\mathbf{P} \mathbf{P}^H \mathbb{E} \left[\tilde{\mathbf{G}}^* \tilde{\mathbf{G}}^T \right] \right) \right] + \mathbf{R}_n, \quad (11)$$

where \mathbf{R}_n is the covariance matrix of the noise. Assuming that the error in the channel estimate has zero mean, we have

$$\begin{aligned} T_1 = & K - f_\tau^{-1} \left(\text{tr} \left(\hat{\mathbf{G}}^T \mathbf{P} \right) + \text{tr} \left(\mathbf{P}^H \hat{\mathbf{G}}^* \right) \right) \\ & + f_\tau^{-2} \left(\text{tr} \left(\mathbf{P}^H \hat{\mathbf{G}}^* \hat{\mathbf{G}}^T \mathbf{P} \right) + \text{tr} \left(\mathbf{P}^H \mathbb{E} \left[\tilde{\mathbf{G}}^* \tilde{\mathbf{G}}^T \right] \mathbf{P} \right) \right) \\ & + f_\tau^{-2} \text{tr} \left(\mathbf{R}_n \right), \end{aligned} \quad (12)$$

where $f_\tau = f\tau$.

The average power of the multiuser interference due to the imperfect CSIT is

$$\mathbb{E} \left[\left\| \tilde{\mathbf{G}}^T \mathbf{P} \right\|^2 \right] = \frac{1}{\tau^2} \text{tr} \left(\mathbb{E} \left[\tilde{\mathbf{G}}^* \tilde{\mathbf{G}}^T \right] \mathbf{P} \mathbf{P}^H \right). \quad (13)$$

Constructing the Lagrangian, we obtain

$$\begin{aligned} \mathcal{L}(\mathbf{P}, f, \lambda) = & K - f_\tau^{-1} \left(\text{tr} \left(\hat{\mathbf{G}}^T \mathbf{P} \right) + \text{tr} \left(\mathbf{P}^H \hat{\mathbf{G}}^* \right) \right) + f_\tau^{-2} \text{tr} \left(\mathbf{R}_n \right) \\ & + f_\tau^{-2} \left(\text{tr} \left(\mathbf{P}^H \hat{\mathbf{G}}^* \hat{\mathbf{G}}^T \mathbf{P} \right) + \text{tr} \left(\mathbf{P}^H \mathbb{E} \left[\tilde{\mathbf{G}}^* \tilde{\mathbf{G}}^T \right] \mathbf{P} \right) \right) \\ & + \frac{1}{\tau^2} \text{tr} \left(\mathbb{E} \left[\tilde{\mathbf{G}}^* \tilde{\mathbf{G}}^T \right] \mathbf{P} \mathbf{P}^H \right) + \lambda \left(\text{tr} \left(\mathbf{P} \mathbf{P}^H \right) - P_t \right). \end{aligned} \quad (14)$$

To solve (14), we first compute the derivatives, resulting in

$$\begin{aligned} \frac{\partial \mathcal{L}(\mathbf{P}, f, \lambda)}{\partial \mathbf{P}^*} = & -f_\tau^{-1} \hat{\mathbf{G}}^* + f_\tau^{-2} \left(\hat{\mathbf{G}}^* \hat{\mathbf{G}}^T + \mathbb{E} \left[\tilde{\mathbf{G}}^* \tilde{\mathbf{G}}^T \right] \right) \mathbf{P} \\ & + \frac{1}{\tau^2} \mathbb{E} \left[\tilde{\mathbf{G}}^* \tilde{\mathbf{G}}^T \right] \mathbf{P} + \lambda \mathbf{P}. \end{aligned} \quad (15)$$

$$\begin{aligned} \frac{\partial \mathcal{L}(\mathbf{P}, f, \lambda)}{\partial f} = & f_\tau^{-2} \left(\text{tr} \left(\hat{\mathbf{G}}^T \mathbf{P} \right) + \text{tr} \left(\mathbf{P}^H \hat{\mathbf{G}}^* \right) \right) - \frac{2}{f^3} \text{tr} \left(\mathbf{R}_n \right) \\ & - \frac{2}{\tau^2 f^3} \text{tr} \left(\mathbf{P}^H \mathbb{E} \left[\tilde{\mathbf{G}}^* \tilde{\mathbf{G}}^T \right] \mathbf{P} \right) \\ & - \frac{2}{\tau^2 f^3} \text{tr} \left(\mathbf{P}^H \hat{\mathbf{G}}^* \hat{\mathbf{G}}^T \mathbf{P} \right). \end{aligned} \quad (16)$$

Equating (15) to zero and then solving for $f_\tau \hat{\mathbf{G}}^*$, we get

$$f_\tau \hat{\mathbf{G}}^* = \underbrace{\left(\hat{\mathbf{G}}^* \hat{\mathbf{G}}^T + \mathbb{E} \left[\tilde{\mathbf{G}}^* \tilde{\mathbf{G}}^T \right] + f^2 \mathbb{E} \left[\tilde{\mathbf{G}}^* \tilde{\mathbf{G}}^T \right] + \lambda f_\tau^2 \mathbf{I} \right)}_{\mathbf{P}^{(i)}} \mathbf{P}. \quad (17)$$

Then, we can isolate \mathbf{P} to obtain the robust precoder. This concludes the proof. \blacksquare

Proposition 2. The parameter λ is computed as

$$\lambda = \frac{\text{tr} \left(\mathbf{R}_n \right)}{f^2 P_t} - \frac{\text{tr} \left(\mathbf{P}^H \mathbb{E} \left[\tilde{\mathbf{G}}^* \tilde{\mathbf{G}}^T \right] \mathbf{P} \right)}{\tau^2 P_t}. \quad (18)$$

Proof: Equating (16) to zero and rearranging terms, we get

$$f_\tau \text{tr} \left(\hat{\mathbf{G}}^* \mathbf{P}^H \right) = \text{tr} \left(\mathbf{P}^H \hat{\mathbf{G}}^* \hat{\mathbf{G}}^T \mathbf{P} \right) + \text{tr} \left(\mathbf{P}^H \mathbb{E} \left[\tilde{\mathbf{G}}^* \tilde{\mathbf{G}}^T \right] \mathbf{P} \right) + \tau^2 \text{tr} \left(\mathbf{R}_n \right). \quad (19)$$

Multiplying the right-hand side of (17) by \mathbf{P}^H and taking the trace results in

$$\begin{aligned} f_\tau \text{tr} \left(\hat{\mathbf{G}}^* \mathbf{P}^H \right) = & \text{tr} \left(\left(\hat{\mathbf{G}}^* \hat{\mathbf{G}}^T + (1 + f^2) \mathbb{E} \left[\tilde{\mathbf{G}}^* \tilde{\mathbf{G}}^T \right] + \lambda f_\tau^2 \mathbf{I} \right) \mathbf{P} \mathbf{P}^H \right). \end{aligned} \quad (20)$$

Equating (19) and (20) gives

$$\tau^2 \text{tr} \left(\mathbf{R}_n \right) = f^2 \text{tr} \left(\mathbb{E} \left[\tilde{\mathbf{G}}^* \tilde{\mathbf{G}}^T \right] \right) + \lambda \tau^2 f^2 \underbrace{\text{tr} \left(\mathbf{P} \mathbf{P}^H \right)}_{P_t} \quad (21)$$

Solving (21) for λ concludes the proof. \blacksquare

Proposition 3. The parameter f is given by

$$f = \frac{1}{\tau} \sqrt{\frac{P_t}{\text{tr} \left(\bar{\mathbf{P}} \bar{\mathbf{P}}^H \right)}} \quad (22)$$

Proof: Substituting the robust precoder into the power constraint results in

$$\begin{aligned} P_t = & \text{tr} \left(\mathbf{P}^{(r)} \mathbf{P}^{(r)H} \right) \\ = & f^2 \tau^2 \text{tr} \left(\bar{\mathbf{P}} \bar{\mathbf{P}}^H \right). \end{aligned} \quad (23)$$

Solving for f concludes the proof. \blacksquare

Note that \mathbf{P} depends on λ and vice-versa. To obtain both quantities, we employ an alternating optimization framework, where one of the variables is fixed to compute the other. We begin the computations with the conventional MMSE as the initial state. With this initial precoder, we update the parameter λ . Algorithm 1 summarizes these steps.

Algorithm 1 Robust MMSE

Input: $P_t, \sigma_n^2, \sigma_e^2, i_t$

Output: $\mathbf{P}^{(r)}$

- 1: $\Theta \leftarrow \mathbb{E} \left[\tilde{\mathbf{G}}^* \tilde{\mathbf{G}}^T \right] = \sigma_e^2 \mathbf{I}$
 - 2: $\bar{\mathbf{P}} [0] \leftarrow \left(\hat{\mathbf{G}}^* \hat{\mathbf{G}}^T + \frac{K \sigma_e^2}{P_t} \mathbf{I} \right)^{-1} \hat{\mathbf{G}}^*$
 - 3: $f [0] \leftarrow \sqrt{\frac{P_t}{\text{tr} \left(\bar{\mathbf{P}} [0] \bar{\mathbf{P}}^H [0] \right)}}$
 - 4: $\mathbf{P} [0] \leftarrow f [0] \bar{\mathbf{P}} [0]$
 - 5: $\lambda [0] \leftarrow \frac{\text{tr} \left(\mathbf{R}_n \right)}{f^2 [0] P_t} - \frac{\text{tr} \left(\mathbf{P} [0] \mathbf{P}^H [0] \mathbb{E} \left[\tilde{\mathbf{G}}^* \tilde{\mathbf{G}}^T \right] \right)}{P_t}$
 - 6: **for** $i = 1 : i_t$ **do**
 - 7: $\bar{\mathbf{P}} [i] \leftarrow \left(\hat{\mathbf{G}}^* \hat{\mathbf{G}}^T + (1 + f^2 [i-1]) \mathbb{E} \left[\tilde{\mathbf{G}}^* \tilde{\mathbf{G}}^T \right] \right. \\ \left. + \lambda [i-1] f^2 [i-1] \mathbf{I} \right)^{-1} \hat{\mathbf{G}}^*$
 - 8: $f [i] \leftarrow \sqrt{\frac{P_t}{\text{tr} \left(\bar{\mathbf{P}} [i] \bar{\mathbf{P}}^H [i] \right)}}$
 - 9: $\mathbf{P} [i] \leftarrow f [i] \bar{\mathbf{P}} [i]$
 - 10: $\lambda [i] \leftarrow \frac{\text{tr} \left(\mathbf{R}_n \right)}{f^2 [i] P_t} - \frac{\text{tr} \left(\mathbf{P} [i] \mathbf{P}^H [i] \mathbb{E} \left[\tilde{\mathbf{G}}^* \tilde{\mathbf{G}}^T \right] \right)}{P_t}$
 - 11: **end for**
 - 12: $\mathbf{P}^{(r)} \leftarrow \mathbf{P} [i_t]$
 - return** $\mathbf{P}^{(r)}$
-

III. ROBUST PRECODERS

To reduce the signaling load of the system and the computational complexity of NW precoders, we propose user-centric cluster-based precoders. To this end, clusters of APs and users are formed. These clusters are defined based on the large-scale channel coefficients given by $\zeta_{k,n}$. The motivation behind this selection scheme is that only small subsets of APs transmit the most relevant signals for reception. The benefit is that we discard the APs whose processing is cost-ineffective and reduce the signaling load.

A. AP selection

To reduce the signaling load, AP selection is performed, so that each user is served only by a subset of APs. The AP selection process is carried out by taking the largest large-scale fading coefficients in the channel. For instance, let us denote by L the number of selected APs. Then, for an arbitrary user, say k -th user, the L APs with the largest large-scale fading coefficient are selected and gathered in the set \mathcal{U}_k . In this sense, we employ the equivalent channel estimate $\mathbf{G}^T = [\bar{\mathbf{g}}_1, \bar{\mathbf{g}}_2, \dots, \bar{\mathbf{g}}_k]^T \in \mathbb{C}^{K \times N}$, which is a sparse matrix with the (n, k) -th element as

$$\bar{\mathbf{g}}_{k,n} = \begin{cases} \hat{g}_{k,n}, & n \in \mathcal{U}_k, \\ 0, & \text{otherwise.} \end{cases} \quad (24)$$

B. Sparse robust MMSE

We employ the equivalent channel estimate $\bar{\mathbf{G}}^T$ to find a robust precoder that reduces the signaling load. It follows that the sparse robust MMSE (MMSE-RB-SP) is

$$\mathbf{P}^{(\text{sp})} = f_\tau \bar{\mathbf{P}}^{(\text{sp})}, \quad (25)$$

where

$$\bar{\mathbf{P}}^{(\text{sp})} = \left(\bar{\mathbf{G}}^* \bar{\mathbf{G}}^T + (1 + f^2) \mathbb{E} \left[\tilde{\mathbf{G}}^* \tilde{\mathbf{G}}^T \right] + \lambda f_\tau^2 \mathbf{I} \right)^{-1} \bar{\mathbf{G}}^*. \quad (26)$$

Then, we resort to the alternating optimization framework described in Algorithm 1 by substituting (26) in (18) to find the parameter λ . Once the parameter λ is obtained, we update the precoder in (26).

C. Cluster-based robust MMSE

One major disadvantage of the MMSE-RB-SP is that it requires the inversion of multiple matrices, which results in high computational cost. To tackle this problem, we group the users in K clusters. Each cluster computes one column of the precoding matrix by employing a channel matrix with reduced dimensions thereby bringing down the computational cost.

Denote by \mathcal{U}_k the cluster of users formed to compute the precoder of the k -th user, i.e., \mathbf{p}_k . User i is included in \mathcal{U}_k if it shares at least N_a antennas with user k , where N_a is a prefixed parameter. In other words, there are N_a antennas providing service to both users, user i and user k . With \mathcal{U}_k defined, we have the reduced dimension matrix of $\hat{\mathbf{G}}$ as $\hat{\mathbf{G}}_k \in \mathbb{C}^{|\mathcal{U}_k| \times K}$.

For this purpose, we define $\mathbf{U}_k \in \mathbb{R}^{|\mathcal{U}_k| \times K}$, which can be interpreted as a user selection matrix. The first row of \mathbf{U}_k is

$$\mathbf{u}_{1,k} = [\underbrace{0, \dots, 0}_{i-1 \text{ terms}}, 1, \dots, 0] \in \mathbb{R}^{|\mathcal{U}_k|}, \quad (27)$$

where $i = \min_{r \in \mathcal{U}_k} r$. Similarly, the second row $\mathbf{u}_{2,k}$ has a one at the l -th position, where l is the second lowest index in \mathcal{U}_k . All the other coefficients of the second row are equal to zero. We similarly obtain the following rows of \mathbf{U}_k . Thus, the reduced matrix is $\hat{\mathbf{G}}_k^T = \mathbf{U}_k \hat{\mathbf{G}}^T$.

We denote the robust precoder that employs a channel matrix with reduced dimensions to compute its columns as MMSE-RB-RD. To find the MMSE-RB-RD, we first solve the following optimization problem

$$\begin{aligned} \{\mathbf{P}', f_k\} = \underset{T_1}{\text{argmin}} \quad & \mathbb{E} [\| \mathbf{s}_k - f_k^{-1} \mathbf{y}_k \|^2] + \mathbb{E} [\| \mathbf{\Delta}_k \|^2] \\ \text{subject to} \quad & \mathbb{E} [\| \mathbf{x}_k \|^2] = \text{tr}(\mathbf{P}' \mathbf{P}'^H) = \frac{|\mathcal{U}_k| P_t}{K}, \end{aligned} \quad (28)$$

Following Proposition 1, the solution to (28) is

$$\mathbf{P}' = f_\tau \bar{\mathbf{P}}', \quad (29)$$

where

$$\bar{\mathbf{P}}' = \left(\hat{\mathbf{G}}_k^* \hat{\mathbf{G}}_k^T + (1 + f^2) \mathbb{E} \left[\tilde{\mathbf{G}}_k^* \tilde{\mathbf{G}}_k^T \right] + \lambda_k f_\tau^2 \mathbf{I} \right)^{-1} \hat{\mathbf{G}}_k^*, \quad (30)$$

Furthermore, using Proposition 2 and Proposition 3, we obtain

$$\lambda_k = \frac{K \text{tr}(\mathbf{R}_{\mathbf{n},k})}{f^2 |\mathcal{U}_k| P_t} - \frac{K \text{tr}(\mathbf{P}'^H \mathbb{E} [\tilde{\mathbf{G}}_k^* \tilde{\mathbf{G}}_k^T] \mathbf{P}')}{\tau^2 |\mathcal{U}_k| P_t}, \quad (31)$$

$$f = \frac{1}{\tau} \sqrt{\frac{|\mathcal{U}_k| P_t}{K \text{tr}(\mathbf{P}' \mathbf{P}'^H)}}. \quad (32)$$

Note that \mathcal{U}_k is associated to decoding of symbol s_k but has reduced dimensions. Therefore, we need an index mapping to find the correct precoder for s_k . Since s_k will be decoded, we find the index q , so that $\mathbf{u}_{q,k}$ contains a one in its k -th entry. It follows that the q -th column of \mathbf{P}' should be employed in $\mathbf{P}^{(\text{MMSE-RB-RD})} = [\mathbf{p}'_1 \dots \mathbf{p}'_k \dots \mathbf{p}'_K]$ i.e.,

$$\mathbf{p}'_k = \left[\mathbf{P}'_k \right]_q. \quad (33)$$

IV. ERGODIC SUM-RATE

To evaluate the performance of the proposed robust precoders, we employ the ergodic sum-rate (ESR) defined as

$$S_r = \mathbb{E} \left[\sum_{k=1}^K \bar{R}_k \right], \quad (34)$$

where $\bar{R}_k = \mathbb{E} [R_k | \hat{\mathbf{G}}]$ is the average rate and R_k is the instantaneous rate of the k -th user. The rate \bar{R}_k averages

out the effects of the imperfect CSIT. Considering Gaussian codebooks, the instantaneous rate is

$$R_k = \log_2(1 + \gamma_k), \quad (35)$$

where γ_k is the signal-to-interference-plus-noise ratio (SINR) at user k .

To obtain γ_k , we compute the mean power at the k -th receiver as

$$\begin{aligned} \mathbb{E}[|y_k|^2] &= \mathbb{E}[y_k^* y_k] \\ &= \frac{1}{\tau^2} \mathbb{E}[s_k^* s_k |\mathbf{g}_k^T \mathbf{p}_k|^2] + \mathbb{E}[n_k^* n_k] \\ &\quad + \frac{1}{\tau^2} \mathbb{E} \left[\sum_{\substack{i=1 \\ i \neq k}}^K s_i^* s_i |\mathbf{g}_k^T \mathbf{p}_i|^2 \right]. \end{aligned} \quad (36)$$

Simplifying $\mathbb{E}[|y_k|^2]$ gives

$$\begin{aligned} \mathbb{E}[|y_k|^2] &= \frac{1}{\tau^2} |(\hat{\mathbf{g}}_k^T - \tilde{\mathbf{g}}_k^T) \mathbf{p}_k|^2 + \sigma_n^2 \\ &\quad + \frac{1}{\tau^2} \sum_{\substack{i=1 \\ i \neq k}}^K a_i^2 |(\hat{\mathbf{g}}_k^T - \tilde{\mathbf{g}}_k^T) \mathbf{p}_i|^2. \end{aligned} \quad (37)$$

Therefore, we have

$$\gamma_k = \frac{|\hat{\mathbf{g}}_k^T \mathbf{p}_k|^2}{d_g + \sum_{\substack{i=1 \\ i \neq k}}^K |(\hat{\mathbf{g}}_k^T - \tilde{\mathbf{g}}_k^T) \mathbf{p}_i|^2 + \tau^2 \sigma_n^2}, \quad (38)$$

where $d_g = |\tilde{\mathbf{g}}_k^T \mathbf{p}_k|^2 - 2\Re\{(\hat{\mathbf{g}}_k^T \mathbf{p}_k)^* (\tilde{\mathbf{g}}_k^T \mathbf{p}_k)\}$.

V. NUMERICAL EXPERIMENTS

We evaluate the performance of the proposed robust precoders via numerical experiments. Throughout all experiments, the large scale fading coefficients are set to

$$\zeta_{k,n} = P_{k,n} \cdot 10^{\frac{\sigma^{(s)} z_{k,n}}{10}}, \quad (39)$$

where $P_{k,n}$ is the path loss and shadowing effect is included in the scalar $10^{\frac{\sigma^{(s)} z_{k,n}}{10}}$ with $\sigma^{(s)} = 8$. The random variable $z_{k,n}$ follows Gaussian distribution with zero mean and unit variance. The path loss was obtained by employing the three-slope model:

$$P_{n,k} = \begin{cases} -L - 35 \log_{10}(d_{n,k}), & d_{n,k} > d_1 \\ -L - 15 \log_{10}(d_1) - 20 \log_{10}(d_{n,k}), & d_0 < d_{n,k} \leq d_1 \\ -L - 15 \log_{10}(d_1) - 20 \log_{10}(d_0), & \text{otherwise,} \end{cases} \quad (40)$$

where $d_{n,k}$ is the distance between the n -th AP and k -th user, $d_1 = 50$ m, $d_0 = 10$ m. The attenuation L is

$$\begin{aligned} L &= 46.3 + 33.9 \log_{10}(f) - 13.82 \log_{10}(h_{\text{AP}}) \\ &\quad - (1.1 \log_{10}(f) - 0.7) h_u + (1.56 \log_{10}(f) - 0.8), \end{aligned} \quad (41)$$

where $h_{\text{AP}} = 15$ m and $h_u = 1.65$ m are the positions of the APs and UEs above the ground, respectively. The carrier frequency was set to $f = 1900$ MHz. The noise variance is

$$\sigma_n^2 = T_o k_B B N_f, \quad (42)$$

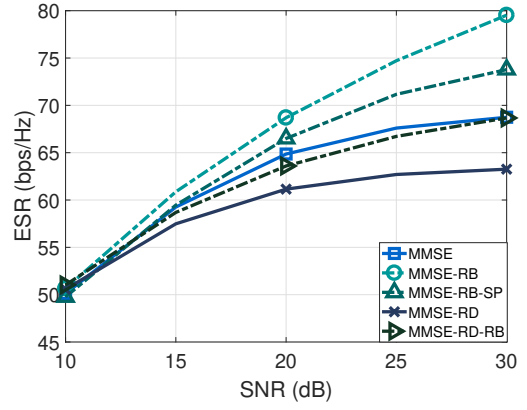


Fig. 1. Sum-rate performance of the proposed robust precoders. Here, $M = 128$, $K = 16$.

where $T_o = 290$ K is the noise temperature, $k_B = 1.381 \times 10^{-23}$ J/K is the Boltzmann constant, $B = 50$ MHz is the bandwidth and $N_f = 10$ dB is the noise figure. The signal-to-noise (SNR) is given by

$$\text{SNR} = \frac{P_t \text{Tr}(\mathbf{G}^T \mathbf{G}^*)}{NK \sigma_n^2}. \quad (43)$$

In all simulations, we consider a total of 128 APs providing service to 16 users. The APs and the users were randomly distributed. To compute the average rate, we employ 100 different error matrices $\tilde{\mathbf{G}}$. Moreover, we considered a total of 100 channel estimates, which results in 10,000 trials to compute the ESR.

Fig. 1 shows the sum-rate performance of the proposed robust precoders compared with the conventional MMSE precoder. The best performance is obtained by robust MMSE (MMSE-RB). The sparse robust MMSE (MMSE-RB-SP) and the robust MMSE with reduced dimensions (MMSE-RB-RD) exhibit a performance loss with respect to the MMSE-RB with the benefit of a lower computational complexity and signaling load.

Next, we assess the sum-rate performance at a SNR of 15 dB for different CSIT qualities (Fig. 2). The proposed MMSE-RD-RB outperforms the conventional MMSE-RD. In general, the proposed robust MMSE techniques outperform the conventional MMSE-based precoders. It follows from Fig. 2 that our proposed techniques are effective against CSIT uncertainties.

VI. SUMMARY

We developed robust MMSE-based precoding techniques for CF-MIMO system. The proposed techniques show a higher tolerance to the imperfections that arise naturally in the CSIT estimate. The proposed MMSE-RB-SP and MMSE-RB-RD have lower computational complexity and signaling load. This allows the implementation of scalable systems but at the expense of sum-rate performance.

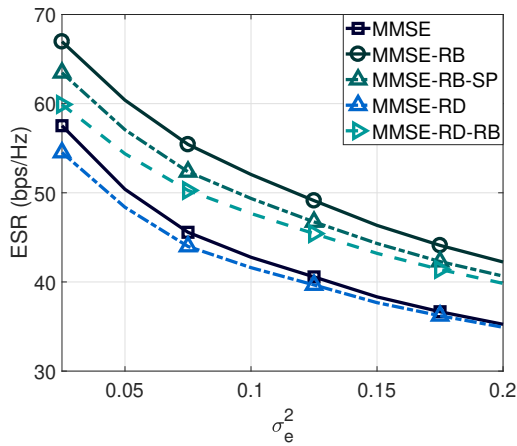


Fig. 2. Sum-rate performance vs channel quality of the proposed robust precoders. Here, $M = 128$, $K = 16$.

REFERENCES

- [1] H. Tataria, M. Shafi, A. F. Molisch, M. Dohler, H. Sjöland, and F. Tufvesson, "6G wireless systems: Vision, requirements, challenges, insights, and opportunities," *Proceedings of the IEEE*, vol. 109, no. 7, pp. 1166–1199, 2021.
- [2] M. Giordani, M. Polese, M. Mezzavilla, S. Rangan, and M. Zorzi, "Toward 6G networks: Use cases and technologies," *IEEE Communications Magazine*, vol. 58, no. 3, pp. 55–61, 2020.
- [3] R. C. de Lamare, "Massive mimo systems: Signal processing challenges and future trends," *URSI Radio Science Bulletin*, vol. 2013, no. 347, pp. 8–20, 2013.
- [4] W. Zhang, H. Ren, C. Pan, M. Chen, R. C. de Lamare, B. Du, and J. Dai, "Large-scale antenna systems with ul/dl hardware mismatch: Achievable rates analysis and calibration," *IEEE Transactions on Communications*, vol. 63, no. 4, pp. 1216–1229, 2015.
- [5] H. A. Ammar, R. Adve, S. Shahbazpanahi, G. Boudreau, and K. V. Srinivas, "User-centric cell-free massive MIMO networks: A survey of opportunities, challenges and solutions," *IEEE Communications Surveys & Tutorials*, vol. 24, no. 1, pp. 611–652, 2022.
- [6] S. Elhoushy, M. Ibrahim, and W. Hamouda, "Cell-free massive MIMO: A survey," *IEEE Communications Surveys & Tutorials*, vol. 24, no. 1, pp. 492–523, 2022.
- [7] H. Yang and T. L. Marzetta, "Energy efficiency of massive MIMO: Cell-free vs. cellular," in *IEEE Vehicular Technology Conference - Spring*, 2018.
- [8] S. Elhoushy and W. Hamouda, "Towards high data rates in dynamic environments using hybrid cell-free massive MIMO/small-cell system," *IEEE Wireless Communications Letters*, vol. 10, no. 2, pp. 201–205, 2021.
- [9] S. Mashdour, R. C. de Lamare, and J. P. S. H. Lima, "Enhanced subset greedy multiuser scheduling in clustered cell-free massive mimo systems," *IEEE Comm. Letters*, vol. 27, no. 2, pp. 610–614, 2022.
- [10] S. Mashdour, S. Salehi, R. C. de Lamare, A. Schmeink, and J. P. S. H. Lima, "Clustering and scheduling with fairness based on information rates for cell-free mimo networks," *IEEE Wireless Communications Letters*, pp. 1–1, 2024.
- [11] H. Q. Ngo, L.-N. Tran, T. Q. Duong, M. Matthaiou, and E. G. Larsson, "On the total energy efficiency of cell-free massive MIMO," *IEEE Transactions on Green Communications and Networking*, vol. 2, no. 1, pp. 25–39, 2018.
- [12] J. Zhang, S. Chen, Y. Lin, J. Zheng, B. Ai, and L. Hanzo, "Cell-free massive MIMO: A new next-generation paradigm," *IEEE Access*, vol. 7, pp. 99 878–99 888, 2019.
- [13] S.-N. Jin, D.-W. Yue, and H. H. Nguyen, "Spectral and energy efficiency in cell-free massive MIMO systems over correlated Rician fading," *IEEE Systems Journal*, vol. 15, no. 2, pp. 2822–2833, 2021.
- [14] M. Joham, W. Utschick, and J. Nosssek, "Linear transmit processing in mimo communications systems," *IEEE Transactions on Signal Processing*, vol. 53, no. 8, pp. 2700–2712, 2005.
- [15] Y. Cai, R. C. d. Lamare, and R. Fa, "Switched interleaving techniques with limited feedback for interference mitigation in ds-cdma systems," *IEEE Transactions on Communications*, vol. 59, no. 7, pp. 1946–1956, 2011.
- [16] K. Zu, R. C. de Lamare, and M. Haardt, "Generalized design of low-complexity block diagonalization type precoding algorithms for multiuser mimo systems," *IEEE Transactions on Communications*, vol. 61, no. 10, pp. 4232–4242, 2013.
- [17] W. Zhang, R. C. de Lamare, C. Pan, M. Chen, J. Dai, B. Wu, and X. Bao, "Widely linear precoding for large-scale mimo with iqi: Algorithms and performance analysis," *IEEE Transactions on Wireless Communications*, vol. 16, no. 5, pp. 3298–3312, 2017.
- [18] S. F. B. Pinto and R. C. de Lamare, "Block diagonalization precoding and power allocation for multiple-antenna systems with coarsely quantized signals," *IEEE Transactions on Communications*, vol. 69, no. 10, pp. 6793–6807, 2021.
- [19] A. R. Flores, R. C. de Lamare, and B. Clerckx, "Linear precoding and stream combining for rate splitting in multiuser mimo systems," *IEEE Communications Letters*, vol. 24, no. 4, pp. 890–894, 2020.
- [20] K. Zu, R. C. de Lamare, and M. Haardt, "Multi-branch tomlinson-harashima precoding design for mu-mimo systems: Theory and algorithms," *IEEE Transactions on Communications*, vol. 62, no. 3, pp. 939–951, 2014.
- [21] L. Zhang, Y. Cai, R. C. de Lamare, and M. Zhao, "Robust multibranch Tomlinson–Harashima precoding design in amplify-and-forward MIMO relay systems," *IEEE Transactions on Communications*, vol. 62, no. 10, pp. 3476–3490, 2014.
- [22] A. R. Flores, R. C. De Lamare, and B. Clerckx, "Tomlinson-Harashima precoded rate-splitting with stream combiners for MU-MIMO systems," *IEEE Transactions on Communications*, vol. 69, no. 6, pp. 3833–3845, 2021.
- [23] L. T. N. Landau and R. C. de Lamare, "Branch-and-bound precoding for multiuser mimo systems with 1-bit quantization," *IEEE Wireless Communications Letters*, vol. 6, no. 6, pp. 770–773, 2017.
- [24] V. M. T. Palhares, A. R. Flores, and R. C. de Lamare, "Robust MMSE precoding and power allocation for cell-free massive MIMO systems," *IEEE Transactions on Vehicular Technology*, vol. 70, no. 5, pp. 5115–5120, 2021.
- [25] P. Clarke and R. C. de Lamare, "Transmit diversity and relay selection algorithms for multirelay cooperative mimo systems," *IEEE Transactions on Vehicular Technology*, vol. 61, no. 3, pp. 1084–1098, 2012.
- [26] V. M. Palhares, R. C. de Lamare, A. R. Flores, and L. T. Landau, "Iterative ap selection, mmse precoding and power allocation in cell-free massive mimo systems," *IET Communications*, vol. 14, no. 22, pp. 3996–4006, 2020. [Online]. Available: <https://ietresearch.onlinelibrary.wiley.com/doi/abs/10.1049/iet-com.2020.0627>
- [27] V. M. T. Palhares, A. R. Flores, and R. C. de Lamare, "Robust mmse precoding and power allocation for cell-free massive mimo systems," *IEEE Transactions on Vehicular Technology*, vol. 70, no. 5, pp. 5115–5120, 2021.
- [28] A. R. Flores and R. C. de Lamare, "Robust and adaptive power allocation techniques for rate splitting based mu-mimo systems," *IEEE Transactions on Communications*, vol. 70, no. 7, pp. 4656–4670, 2022.
- [29] A. R. Flores, R. C. de Lamare, and K. V. Mishra, "Clustered cell-free multi-user multiple-antenna systems with rate-splitting: Precoder design and power allocation," *IEEE Transactions on Communications*, vol. 71, no. 10, pp. 5920–5934, 2023.
- [30] Y. Cai, R. C. de Lamare, L.-L. Yang, and M. Zhao, "Robust mmse precoding based on switched relaying and side information for multiuser mimo relay systems," *IEEE Transactions on Vehicular Technology*, vol. 64, no. 12, pp. 5677–5687, 2015.
- [31] H. Ruan and R. C. de Lamare, "Distributed robust beamforming based on low-rank and cross-correlation techniques: Design and analysis," *IEEE Transactions on Signal Processing*, vol. 67, no. 24, pp. 6411–6423, 2019.
- [32] D. M. V. Melo, L. T. N. Landau, R. C. de Lamare, P. F. Neuhaus, and G. P. Fettweis, "Zero-crossing precoding techniques for channels with 1-bit temporal oversampling adcs," *IEEE Transactions on Wireless Communications*, vol. 22, no. 8, pp. 5321–5336, 2023.
- [33] E. Nayebi, A. Ashikhmin, T. L. Marzetta, H. Yang, and B. D. Rao, "Precoding and power optimization in cell-free massive MIMO systems," *IEEE Transactions on Wireless Communications*, vol. 16, no. 7, pp. 4445–4459, 2017.
- [34] E. Björnson and L. Sanguinetti, "Making cell-free massive MIMO competitive with MMSE processing and centralized implementation,"

- IEEE Transactions on Wireless Communications*, vol. 19, no. 1, pp. 77–90, 2020.
- [35] H. Q. Ngo, A. Ashikhmin, H. Yang, E. G. Larsson, and T. L. Marzetta, “Cell-free massive MIMO versus small cells,” *IEEE Transactions on Wireless Communications*, vol. 16, no. 3, pp. 1834–1850, 2017.
- [36] E. Björnson and L. Sanguinetti, “Scalable cell-free massive MIMO systems,” *IEEE Transactions on Communications*, vol. 68, no. 7, pp. 4247–4261, 2020.
- [37] S. Buzzi, C. D’Andrea, A. Zappone, and C. D’Elia, “User-centric 5G cellular networks: Resource allocation and comparison with the cell-free massive MIMO approach,” *IEEE Transactions on Wireless Communications*, vol. 19, no. 2, pp. 1250–1264, 2020.
- [38] A. R. Flores, R. C. de Lamare, and K. V. Mishra, “Clustered cell-free multi-user multiple-antenna systems with rate-splitting: Precoder design and power allocation,” *IEEE Transactions on Communications*, vol. 71, no. 10, pp. 5920–5934, 2023.
- [39] V. M. Palhares, R. C. de Lamare, A. R. Flores, and L. T. Landau, “Iterative AP selection, MMSE precoding and power allocation in cell-free massive MIMO systems,” *IET Communications*, vol. 14, no. 22, pp. 3996–4006, 2020.
- [40] M. M. Mojahedian and A. Lozano, “Subset regularized zero-forcing precoders for cell-free C-RANs,” in *European Signal Processing Conference*, 2021, pp. 915–919.
- [41] A. R. Flores, R. C. de Lamare, and K. V. Mishra, “Cluster precoders for cell-free MU-MIMO systems,” in *IEEE International Symposium on Wireless Communication Systems*, 2022, pp. 1–6.
- [42] M. Vu and A. Paulraj, “MIMO wireless linear precoding,” *IEEE Signal Processing Magazine*, vol. 24, no. 5, pp. 86–105, 2007.
- [43] A. Elnashar, S. M. Elnoubi, and H. A. El-Mikati, “Further study on robust adaptive beamforming with optimum diagonal loading,” *IEEE Transactions on Antennas and Propagation*, vol. 54, no. 12, pp. 3647–3658, 2006.
- [44] O. Besson and F. Vincent, “Performance analysis of beamformers using generalized loading of the covariance matrix in the presence of random steering vector errors,” *IEEE Transactions on Signal Processing*, vol. 53, no. 2, pp. 452–459, 2005.
- [45] S. Vorobyov, A. Gershman, and Z.-Q. Luo, “Robust adaptive beamforming using worst-case performance optimization: A solution to the signal mismatch problem,” *IEEE Transactions on Signal Processing*, vol. 51, no. 2, pp. 313–324, 2003.
- [46] H. Joudeh and B. Clerckx, “Sum-rate maximization for linearly precoded downlink multiuser MISO systems with partial CSIT: A rate-splitting approach,” *IEEE Transactions on Communications*, vol. 64, no. 11, pp. 4847–4861, 2016.
- [47] A. R. Flores, R. C. De Lamare, and K. V. Mishra, “Rate-splitting meets cell-free MIMO communications,” in *IEEE International Conference on Communications Workshops*, 2022, pp. 657–662.
- [48] M. Medra and T. N. Davidson, “Low-complexity robust MISO downlink precoder design with per-antenna power constraints,” *IEEE Transactions on Signal Processing*, vol. 66, no. 2, pp. 515–527, 2018.
- [49] M. Joham, W. Utschick, and J. Nosssek, “Linear transmit processing in MIMO communications systems,” *IEEE Transactions on Signal Processing*, vol. 53, no. 8, pp. 2700–2712, 2005.